Reducing the bias of causality measures

A. Papana* and D. Kugiumtzis†
Department of Mathematical, Physical and Computational Sciences, Faculty of Engineering, Aristotle University of Thessaloniki, Thessaloniki 54124, Greece

P. G. Larsson
Department of Neurology, Oslo University Hospital, Norway

(Received 19 July 2010; revised manuscript received 10 January 2011; published 21 March 2011)

Measures of the direction and strength of the interdependence between two time series are evaluated and modified to reduce the bias in the estimation of the measures, so that they give zero values when there is no causal effect. For this, point shuffling is employed as used in the frame of surrogate data. This correction is not specific to a particular measure and it is implemented here on measures based on state space reconstruction and information measures. The performance of the causality measures and their modifications is evaluated on simulated uncoupled and coupled dynamical systems and for different settings of embedding dimension, time series length, and noise level. The corrected measures, and particularly the suggested corrected transfer entropy, turn out to stabilize at the zero level in the absence of a causal effect and detect correctly the direction of information flow when it is present. The measures are also evaluated on electroencephalograms (EEG) for the detection of the information flow in the brain of an epileptic patient. The performance of the measures on EEG is interpreted in view of the results from the simulation study.

DOI: 10.1103/PhysRevE.83.036207 PACS number(s): 05.45.Tp, 05.45.Ac, 02.70.−c

I. INTRODUCTION

The interaction or coupling between variables or subsystems of a complex dynamical system is a developing area of nonlinear dynamics and time-series analysis [1,2]. The detection and characterization of interdependence among interacting components of complex systems can give information about their functioning and a better understanding of the system dynamics. Information flow is a ubiquitous feature of many complex physical phenomena, such as climatic processes [3,4], electronic circuits [5], financial markets [6], and the brain system [7,8].

Given a set of time-series observations, it is essential to assess whether they originate from coupled or uncoupled systems, estimate the hidden causal dependencies between them, and detect which system is the driver and which is the responder. Granger causality has been the leading approach for a long time for inferring the direction of interactions, based on the predictability of time series using linear models [9]. If prior knowledge of a time series improves the prediction of another, the former Granger causes the latter. Many measures have been developed based on the concept of Granger causality using cross spectra and cross prediction of linear models [10,11]. Granger causality has been extended to incorporate also nonlinear relationships using nonlinear models [12,13], or other model-free measures that exploit nonlinear properties of dynamical systems, such as measures based on phase and event synchronization [14,15], reconstruction of the state spaces [7,16–19], and information theory [1,20–24]. The information measures make no assumptions on the system dynamics, as opposed to phase or event synchronization measures that assume strong oscillatory behavior or distinct event occurrences, respectively, and the state space methods that require local dynamics being preserved in neighborhoods of reconstructed points.

Comparative studies on different causality measures reported in [25–28] are not conclusive and do not point to the same measures, also because different measures are used in each study. In a recent review and evaluation of state space, synchronization, and information causality measures, we stressed the need to render the statistical significance of the causality measures as most measures are biased and indicate causal effects when they are not present [29]. A thorough investigation for the validity and usefulness of a causality measure should start with a test of significance, i.e., a measure should not identify coupling (or interaction) in any direction when it is not present. In statistical terms, this means that the actual probability of rejection of the null hypothesis when it is true does not exceed the nominal significance level, usually set to 0.05. As in any statistical test, power is of interest after the correct significance is established, where power here is related to the sensitivity of the causality measure in detecting interaction and identifying its direction. Some approaches have been proposed to render the significance of the coupling measures using the concept of surrogate data testing. The so-called effective transfer entropy uses a random shuffling of the driving time series [22]. Twin surrogates, generated as shadowing trajectories of the original trajectories, have recently been suggested to preserve the original individual dynamics [30]. Apparently, the closeness of shadowing in the twin surrogates determines the level at which the coupling is destroyed. A different and simple way to generate surrogates is to time-shift one of the two time series, as suggested in [13].

We propose here a different generation of surrogates and shuffle randomly the reconstructed points of the driving time

*agpapana@gen.auth.gr
†dkugiu@gen.auth.gr; URL http://users.auth.gr/dkugiu

series rather than the samples, as is done for the effective transfer entropy. The random shuffling destroys completely the coupling, and the use of the reconstructed points preserves the individual system dynamics, but perhaps not in the same way as the twin or time-shifted surrogates. Instead of making a formal surrogate data test, we use these surrogates to correct the measure and reduce the bias. The performance of the measures of mean conditional probability of recurrence [18], transfer entropy [20], and symbolic transfer entropy [23], as well as the respective surrogate-based corrections, are assessed on multiple realizations of uncoupled and coupled nonlinear systems (maps and flows) for a range of increasing coupling strengths. In the numerical simulations, the detection of the coupling directionality and strength is evaluated at different settings of dynamics complexity, time-series length, noise level, and embedding dimensions for the reconstruction of the two state spaces. All these factors can be sources of bias in the estimation of the causality measures.

The structure of the paper is as follows. The directional coupling measures considered in this study are briefly presented in Sec. II, and the proposed corrections of the measures are presented in Sec. III. The results of the application of the measures and their corrections on simulated systems are discussed in Sec. IV, and those of a real application of EEG recordings from epileptic patients are discussed in Sec. V. Finally, the conclusions are drawn in Sec. VI.

II. CAUSALITY MEASURES

Let $\{x_t\}$ and $\{y_t\}$, $t = 1,\ldots,n$, denote two simultaneously observed time series derived from the dynamical systems X and Y, respectively. We formulate the causality measures for the causal effect of system X on system Y, denoted as $X \to Y$. For the opposite direction $Y \to X$, the formulation is analogous. Let m_x and m_y be the embedding dimensions and τ_x and τ_y the delays for the state space reconstructions of the two systems, respectively, giving the reconstructed points $\mathbf{x}_t = (x_t, x_{t-\tau_x}, \ldots, x_{t-(m_x-1)\tau_x})'$ and $\mathbf{y}_t = (y_t, y_{t-\tau_y}, \ldots, y_{t-(m_y-1)\tau_y})'$, where $t = 1,\ldots,n'$ and $n' = n - \max\{(m_x-1)\tau_x, (m_y-1)\tau_y\}$. The steps ahead or time horizon to address the interaction are denoted by h.

A. Mean conditional probability of recurrence

A state space causality measure based on recurrence quantification analysis [31] was recently introduced; it is termed the mean conditional probability of recurrence [18]. Let

$$R^X_{i,j} = \Theta(\varepsilon_x - \|\mathbf{x}_i - \mathbf{x}_j\|),$$
$$R^Y_{i,j} = \Theta(\varepsilon_y - \|\mathbf{y}_i - \mathbf{y}_j\|), i,j = 1,\ldots,n'$$

be the recurrence matrices of X and Y, respectively, where $\Theta(\cdot)$ is the Heaviside function counting points with distance smaller than the predefined distance thresholds ε_x and ε_y, respectively. The joint recurrence matrix of (X,Y) is defined as

$$J^{X,Y}_{i,j} = \Theta(\varepsilon_x - \|\mathbf{x}_i - \mathbf{x}_j\|)\Theta(\varepsilon_y - \|\mathbf{y}_i - \mathbf{y}_j\|), i, j = 1,\ldots,n',$$

i.e., a joint recurrence occurs if the system X recurs in its own phase space, and simultaneously the system Y recurs also in its own phase space. The mean conditional probability of recurrence (MCR) is defined as

$$M_{X\to Y} = \frac{1}{n'}\sum_{i=1}^{n'} \frac{\sum_{j=1}^{n'} J^{X,Y}_{i,j}}{\sum_{j=1}^{n'} R^Y_{i,j}}. \quad (1)$$

If X drives Y, then $M_{X\to Y} > M_{Y\to X}$. The concept of recurrence has been used to quantify a weaker form of synchronization, and MCR is an extension of it that detects the direction of coupling [18].

B. Transfer entropy

Transfer entropy (TE) quantifies the information flow from X to Y by the amount of information explained in Y at one step ahead (or generally h steps ahead) by the state of X, accounting for the concurrent state of Y [20]. The concept of TE extends the Shannon entropy to transition probabilities and quantifies how the conditioning on X change the transition probabilities of Y. Using the reconstructed points for X and Y as given above, TE is defined as

$$T_{X\to Y} = \sum p(y_{t+h}, \mathbf{x}_t, \mathbf{y}_t) \ln \frac{p(y_{t+h}|\mathbf{x}_t, \mathbf{y}_t)}{p(y_{t+h}|\mathbf{y}_t)}, \quad (2)$$

where $p(y_{t+h}, \mathbf{x}_t, \mathbf{y}_t)$, $p(y_{t+h}|\mathbf{x}_t, \mathbf{y}_t)$, and $p(y_{t+h}|\mathbf{y}_t)$ are the joint and conditional probability mass functions for a proper binning. The time horizon h is introduced here instead of the time step one that was originally used in the definition of TE. TE can also be defined in terms of entropies as

$$T_{X\to Y} = H(\mathbf{x}_t, \mathbf{y}_t) - H(y_{t+h}, \mathbf{x}_t, \mathbf{y}_t) + H(y_{t+h}, \mathbf{y}_t) - H(\mathbf{y}_t). \quad (3)$$

Instead of binning, we define TE in terms of correlation sums as follows. Let X be a continuous, possibly vector-valued, random variable. For a fixed small r, the entropy of a variable X can be estimated as $H(X) \simeq \ln C(\mathbf{x}_t) + m \ln r$ [32], where $C(\mathbf{x}_t)$ is the correlation sum for the vectors $\mathbf{x}_t$ with embedding dimension m [$C(\mathbf{x}_t)$ is an estimate of the probability of points being closer than r]. The standardized Euclidian norm, i.e., the Euclidean distance divided by the square root of the embedding dimension, is used for the calculation of the correlation sum. Let us denote the correlation sums of the vectors $[y_{t+h}, \mathbf{x}_t, \mathbf{y}_t]$, $\mathbf{y}_t$, $[\mathbf{x}_t, \mathbf{y}_t]$, and $[y_{t+h}, \mathbf{y}_t]$ as $C(y_{t+h}, \mathbf{x}_t, \mathbf{y}_t)$, $C(\mathbf{y}_t)$, $C(\mathbf{x}_t, \mathbf{y}_t)$, and $C(y_{t+h}, \mathbf{y}_t)$, respectively. Then, TE is defined as

$$T_{X\to Y} = \ln \frac{C(y_{t+h}, \mathbf{x}_t, \mathbf{y}_t) C(\mathbf{y}_t)}{C(\mathbf{x}_t, \mathbf{y}_t) C(y_{t+h}, \mathbf{y}_t)}. \quad (4)$$

C. Symbolic transfer entropy

Symbolic transfer entropy (STE) is the transfer entropy defined on rank points formed by the reconstructed vectors of X and Y [23]. Thus, for each vector $\mathbf{y}_t$, the ranks of its components assign a rank point $\hat{\mathbf{y}}_t = [r_1, r_2, \ldots, r_{m_y}]$, where $r_j \in \{1,2,\ldots,m_y\}$ for $j = 1,\ldots,m_y$. Following this sample-point to rank-point conversion, the sample y_{t+h} in

Eq. (2) is taken as a rank point at time $t+h$, $\hat{\mathbf{y}}_{t+h}$, and STE is defined as

$$T^S_{X\to Y} = H(\hat{\mathbf{x}}_t,\hat{\mathbf{y}}_t) - H(\hat{\mathbf{y}}_{t+h},\hat{\mathbf{x}}_t,\hat{\mathbf{y}}_t) + H(\hat{\mathbf{y}}_{t+h},\hat{\mathbf{y}}_t) - H(\hat{\mathbf{y}}_t), \tag{5}$$

where the entropies are defined on the rank points.

D. Effective transfer entropy

A modification of TE, called effective transfer entropy (ETE), was defined in [22] as the difference of TE computed on the original bivariate time series and the TE computed on a surrogate bivariate time series, where the driving time series X is randomly shuffled,

$$T^E_{X\to Y} = T_{X\to Y} - T_{X_{\text{shuffled}}\to Y}.$$

The use of a randomly shuffled surrogate aims at setting a significance threshold in the estimation of TE. The approach of ETE can be used for the estimation of any other causal measure. Here, for the estimation of ETE, instead of one random permutation, a number of M random permutations of the driving time series X are considered, and therefore $T_{X_{\text{shuffled}}\to Y}$ in the definition of ETE is replaced by the mean of the corresponding M values,

$$T^E_{X\to Y} = T_{X\to Y} - \frac{1}{M}\sum_{l=1}^{M} T_{X_{l,\text{shuffled}}\to Y}, \tag{6}$$

where $l = 1,\ldots,M$. In the same way, we define effective STE, denoted ESTE (T^{SE}).

E. Relationship of MCR and TE

MCR defines in a rather direct way the conditional probability of close points in Y given they are close in X, whereas most state space methods, such as nonlinear interdependence measures [7,16,17,19], attempt to approximate the conditional probability indirectly through analogy in distances. In this respect, the MCR method is closer to information measures, such as TE. However, TE involves also transition probabilities that can give additional information about the effect of the driving system on the future of the response system.

In [18], it is stressed that MCR requires a smaller number of data points than TE. This is true if binning estimators are used for the probability functions in TE, but for the estimator considered here using correlation sums, the data requirements are the same, because the stability of the estimation in both MCR and TE relies on having good statistics of points in the neighborhoods for a given distance. Certainly, this holds when the distance r in TE and the distances ϵ_x and ϵ_y in MCR are at the same level. It is also mentioned in [18] that TE, but not MCR, may give values larger than zero for both directions when the coupling is purely unidirectional. As we show below, this bias is not specific to a measure and should be attributed to other factors, such as the system complexity and the length of the time series. The fact that MCR did not exhibit this bias in the results in [18] may be due to the optimization of the values of the thresholds ϵ_x and ϵ_y, so that for no coupling both averages of the estimated probabilities of recurrences $p(\mathbf{x}_i)$ and $p(\mathbf{y}_i)$ are equal to 0.01. In our simulations, we do not optimize ϵ_x and ϵ_y but use a fixed $\epsilon_x = \epsilon_y = r$ and have the time series standarized, i.e., the same distance threshold is used in the computation of both MCR and TE in all simulations.

III. MODIFICATIONS OF CAUSALITY MEASURES

A main drawback of all causality measures considered in this study is that they do not provide stable and consistent results, particularly for weak-coupling structures and noisy time series. The measures have bias that may be different in each direction, depending also on the dynamics of each system, the time-series length, and the state space reconstruction. The existence of bias and spurious detection of causal effects have been previously reported for different causality measures [1,25,27,29]. When there is no causal effect, the positive bias may be misinterpreted as weak coupling.

A possible solution to this problem is provided by reducing the bias of the measure using surrogate data. Surrogate time series can be used to rule out spurious conclusions about the existence and the direction of coupling. When testing the null hypothesis that the two time series are uncoupled, the bivariate surrogates should replicate the dynamics of each system and be independent of each other. In this way, the bias due to the individual system dynamics and state space reconstruction is preserved in the surrogates. Here, we do not apply a formal surrogate data test, but we use the surrogate values to correct for the bias of the coupling measure, as shown below.

The approach in ETE attempts to generate surrogates for this purpose by randomizing the temporal structure of the driving time series, so that if the systems are coupled, cause and effect are lost. However, by randomly shuffling a time series, its self-dynamical structure is destroyed as well. We present below a correction to the measures MCR, TE, and STE, based on the frame of surrogates, which are extracted by randomly shuffling the reconstructed vectors of the driving time series to preserve the dynamical properties of each system.

A. Corrected MCR

The corrected MCR (CMCR) defined below aims at reducing the bias of MCR in the case of no causal effects. Recall that the ones at each line i of the joint recurrence matrix $J^{X,Y}_{i,j}$, $i,j = 1,\ldots,n'$, correspond to the matched time indices of the neighboring points to $\mathbf{x}_i$ in system X and the neighboring points to $\mathbf{y}_i$ in system Y, and the number of matches determines the strength of coupling. Thus by randomly shuffling the lines of matrix $R^X_{i,j}$, $i,j = 1,\ldots,n'$, we destroy this match, as for each $\mathbf{y}_i$, the neighbors for the X system no longer regard $\mathbf{x}_i$ but rather another randomly chosen point. Repeating this random shuffling M times, we get M new matrices $Rs^X_{l,i,j}$, $l = 1,\ldots,M$, and M new joint recurrence matrices $Js^{X,Y}_{l,i,j}$. This allows us to take the average number of common neighbors at each time index i over the M realizations with regard to the scenario of no coupling. The "surrogate" MCR is then defined as

$$M^{\text{sur}}_{X\to Y} = \frac{1}{n'}\sum_{i=1}^{n'} \frac{\frac{1}{M}\sum_{l=1}^{M}\sum_{j=1}^{n'} Js^{X,Y}_{l,i,j}}{\sum_{j=1}^{n'} R^Y_{i,j}}$$

and CMCR is

$$M^{C}_{X\to Y} = M_{X\to Y} - M^{\text{sur}}_{X\to Y}. \quad (7)$$

B. Corrected TE and STE

For an estimation of the corrected TE (CTE), the same idea is implemented and we assume again M random shufflings of the points of the X system. Thus in the estimation of TE in Eq. (4), the terms of the correlation sums $C(y_{t+h},\mathbf{x}_t,\mathbf{y}_t)$ and $C(\mathbf{x}_t,\mathbf{y}_t)$ are replaced by the corresponding mean values of the correlation sums estimated on the point shuffled surrogates, given as

$$C_s(y_{t+h},\mathbf{x}_t,\mathbf{y}_t) = \frac{1}{M}\sum_{l=1}^{M} C(y_{t+h},\mathbf{x}_{t_l},\mathbf{y}_t)$$

and

$$C_s(\mathbf{x}_t,\mathbf{y}_t) = \frac{1}{M}\sum_{l=1}^{M} C(\mathbf{x}_{t_l},\mathbf{y}_t),$$

where t_l denotes a random time index and $\mathbf{x}_{t_l}$ is the point in system X at the lth replication for the time index t. Then, the "surrogate" TE value is estimated as

$$T^{\text{sur}}_{X\to Y} = \log\frac{C_s(y_{t+h},\mathbf{x}_t,\mathbf{y}_t)C(\mathbf{y}_t)}{C_s(\mathbf{x}_t,\mathbf{y}_t)C(y_{t+h},\mathbf{y}_t)}$$

and CTE is defined as

$$T^{C}_{X\to Y} = T_{X\to Y} - T^{\text{sur}}_{X\to Y}. \quad (8)$$

Note that instead of taking the average of M "surrogate" TE values as in Eq. (6) for ETE, a single "surrogate" TE value is extracted by taking the average at each term of the expression of TE. The difference is actually in taking the average after or before the logarithm of each correlation sum. The former gives more variable estimates of TE on the surrogates, as for small values of the correlation sums we obtain large negative logarithms. Thus by taking the mean of the correlation sums over all surrogates, we stabilize the correlation sum to the most representative value expected if the systems were to be uncoupled. In turn, this gives a more stable estimation of the mean entropy terms and subsequently the mean transfer entropy for the surrogates.

Substituting in Eq. (8) the expression for the original and surrogate TE, the terms $H(\mathbf{y}_t)$ and $H(y_{t+h},\mathbf{y}_t)$ cancel out and we get

$$T^{C}_{X\to Y} = \log\frac{C(y_{t+h},\mathbf{x}_t,\mathbf{y}_t)C_s(\mathbf{x}_t,\mathbf{y}_t)}{C_s(y_{t+h},\mathbf{x}_t,\mathbf{y}_t)C(\mathbf{x}_t,\mathbf{y}_t)}.$$

This measure should be zero when X does not have any effect on Y. However, other sources of bias may still cause deviations from zero even in the lack of a causal effect, and this will be tested below through simulations.

Corrected STE (CSTE) is defined analogously to CTE, and the expression of CSTE in terms of entropies is

$$T^{SC}_{X\to Y} = H(\hat{\mathbf{x}}_t,\hat{\mathbf{y}}_t) - H(\hat{y}_{t+h},\hat{\mathbf{x}}_t,\hat{\mathbf{y}}_t) - H_s(\hat{\mathbf{x}}_t,\hat{\mathbf{y}}_t) + H_s(\hat{y}_{t+h},\hat{\mathbf{x}}_t,\hat{\mathbf{y}}_t), \quad (9)$$

where

$$H_s(\hat{\mathbf{x}}_t,\hat{\mathbf{y}}_t) = \frac{1}{M}\sum_{l=1}^{M} H(\hat{\mathbf{x}}_{t_l},\hat{\mathbf{y}}_t) \quad (10)$$

and

$$H_s(\hat{y}_{t+h},\hat{\mathbf{x}}_t,\hat{\mathbf{y}}_t) = \frac{1}{M}\sum_{l=1}^{M} H(\hat{y}_{t+h},\hat{\mathbf{x}}_{t_l},\hat{\mathbf{y}}_t). \quad (11)$$

IV. EVALUATION OF CAUSALITY MEASURES ON SIMULATED SYSTEMS

A. Simulation setup

Measures of directional coupling are computed on 100 realizations of the following unidirectionally coupled systems, for increasing coupling strengths and for both directions $X\to Y$ and $Y\to X$.

(i) Two unidirectionally coupled Henon maps,

$$x_{t+1} = 1.4 - x_t^2 + 0.3x_{t-1},$$
$$y_{t+1} = 1.4 - cx_t y_t - (1-c)y_t^2 + 0.3y_{t-1},$$

with coupling strengths $c = 0,0.05,0.1,0.2,0.3,0.4,0.5,0.6,$ and 0.7, whereas the onset to identical synchronization occurs at approximately $c = 0.65$ [14,16].

(ii) Two unidirectionally coupled Mackey-Glass systems [33],

$$\frac{dx}{dt} = \frac{0.2x_{t-\Delta_x}}{1+x^{10}_{t-\Delta_x}} - 0.1x_t,$$
$$\frac{dy}{dt} = \frac{0.2y_{t-\Delta_y}}{1+y^{10}_{t-\Delta_y}} + c\frac{0.2x_{t-\Delta_x}}{1+x^{10}_{t-\Delta_x}} - 0.1y_t \quad (12)$$

for Δ_x and Δ_y taking the values 17, 30, and 100 (all nine combinations for the driving and response system) and with coupling strengths $c = 0$, 0.05, 0.1, 0.15, 0.2, 0.3, 0.4, and 0.5. The choice of the different Δ_x and Δ_y aims at investigating the performance of the measures on systems with the same and different complexity. For the three delay parameters, the Mackey-Glass system is chaotic with a correlation dimension about 2 for $\Delta_x = 17$, 3 for $\Delta_x = 30$, and 7 for $\Delta_x = 100$ [34]. The integration was done with the function dde23 of the MATLAB software, and the time series were obtained with a sampling time of 4 s.

(iii) A coupled nonlinear stochastic system (see [35]),

$$x_t = 3.4x_{t-1}(1-x_{t-1}^2)e^{-x_{t-1}^2} + 0.4e_{1t},$$
$$y_t = 3.4y_{t-1}(1-y_{t-1}^2)e^{-y_{t-1}^2} + 0.5x_{t-1}y_{t-1} + 0.4e_{2t},$$
$$z_t = 3.4z_{t-1}(1-z_{t-1}^2)e^{-z_{t-1}^2} + 0.3y_{t-1} + 0.5x_{t-1}^2 + 0.4e_{3t},$$

where e_{1t}, e_{2t}, and e_{3t} are standard white Gaussian noise processes. We note that the correct directed causal effects are $X\to Y$, $Y\to Z$, and $X\to Z$.

The time-series lengths for the coupled Henon maps are $n = 512,1024,$and2048, and for the Mackey-Glass system, $n = 2048$. Gaussian white noise is also added to these time series with standard deviations 5% and 20% of the standard deviation of the time series. Further, we investigate the dependence of the measures on the state space reconstruction of the two systems. For the coupled Henon system, the embedding dimensions vary as $m_x = 1,\ldots,5$ and $m_y = 1,\ldots,5$. For the coupled Mackey-Glass systems, m_x and m_y vary from 1 and up to 10, depending on the delays of the coupled systems. For symbolic

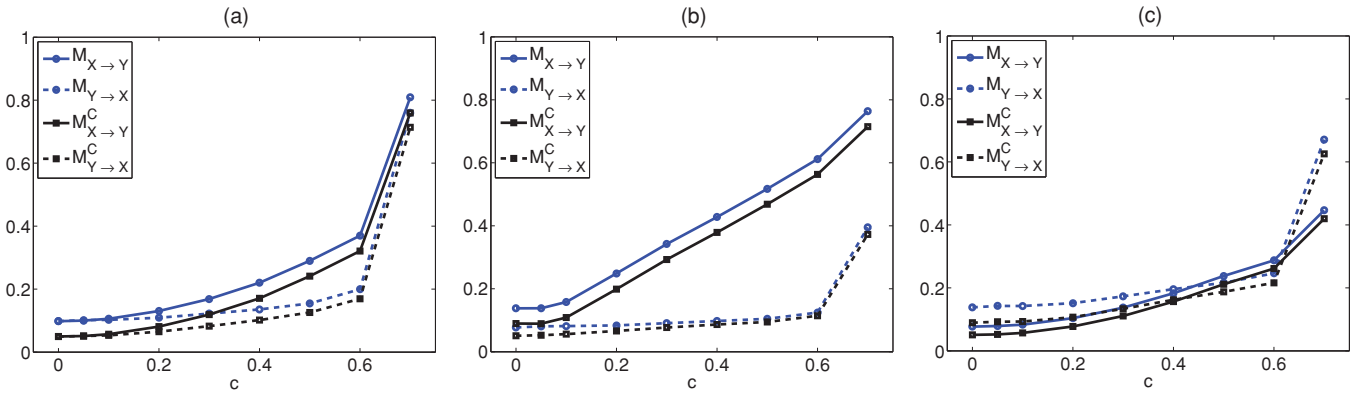

FIG. 1. (Color online) (a) Mean estimated values of MCR (M) and CMCR (M^C) for both directions from 100 realizations of the noise-free unidirectionally coupled Henon map, where $m_x = 2, m_y = 2$, and $n = 512$. (b) and (c) are as in (a), but for $m_x = 2, m_y = 4$ and $m_x = 4, m_y = 2$, respectively.

information measures, the embedding dimensions cannot be set equal to 1 as there will be no different symbolic patterns.

To obtain quantitative summary results for the performance of the measures, t-tests for means are conducted for the following three null hypotheses H_0:

(i) H_0^1: The mean of the measure in the direction $X \to Y$ is zero.

(ii) H_0^2: The mean of the measure for the direction $Y \to X$ is zero.

(iii) H_0^3: The means of the measures in the two directions are equal.

We assume that the distribution of the measure in both directions formed from its values in 100 realizations is normal, and for H_0^3 that they have the same variance, which both seem to be statistically satisfied (as resulted from the Kolmogorov-Smirnov test for normality and the Fisher test for equal variances applied to some of the realizations).

Using as samples the measure values from 100 realizations for each case, the performance of each measure is quantified in terms of the rejection or not of each of the three H_0 at the significance level $\alpha = 0.05$, giving a score of 0 if H_0 is not rejected and 1 if it is rejected. So the total score for all three H_0 ranges from 0 to 3. There are two settings of interest for the coupling of X and Y: no coupling that regards the significance of the measure, for which the best total score is 0, and the presence of unidirectional coupling that regards the discriminating power of the measure, for which the best total score is 2, meaning rejection of H_0^1 and H_0^3 but not H_0^2 (the latter yielding the direction of no causal effect). Note that a score of 2 can also be obtained if in both directions a measure is significantly different from 0 but at the same level. Therefore, we will explicitly name the setting for each H_0 when there is ambiguity from the total score.

B. Results on the unidirectionally coupled Henon maps

MCR and CMCR measures are significantly affected by the embedding dimension, time-series length, and noise level. There are two important problems with MCR: first, it increases also in the opposite direction (with no causal effect) with the increase of the coupling strength, which may erroneously be interpreted as bidirectional coupling, and second, it is positively biased in the uncoupled case ($c = 0$), especially for short time series. By increasing the time-series length and the embedding dimensions, MCR and CMCR both decrease. The corrected measure CMCR obtains always smaller values than MCR in both directions and it is closer to zero for $c = 0$, particularly for small time series and small embedding dimensions (see Fig. 1). Both MCR and CMCR maintain a larger increase in the correct direction of interaction with the coupling strength when $m_x = m_y$, amplify the difference in the two directions when $m_x < m_y$, and decrease this difference or even tend to suggest more interaction in the opposite direction when $m_x > m_y$. The addition of small noise level (5%) does not substantially affect MCR and CMCR, but 20% noise level lowers MCR and CMCR toward the zero level for both directions. In this case, an increase of the embedding dimension regains the correct signature of coupling, but adds positive bias at a level that is clearly seen for $c = 0$.

TE and mainly CTE are found to be more effective in detecting the direction of the information flow than MCR and CMCR. The causal effect is correctly detected in all simulations on the Henon maps. The correct direction is preserved for all combinations of the embedding dimensions except for $m_x = 1$ and $m_y > 1$, where a spurious increase at the direction $Y \to X$ is observed. The CTE measure is always effectively zero for both directions when $c = 0$, whereas TE tends to be positive (at cases deviating significantly from the zero level) and ETE gives negative values and not equal in both directions. Also, ETE is affected by the selection of the embedding dimensions much more than TE and CTE (see Fig. 2).

The three information measures turn out to be robust to noise, and the detection of the direction of interaction gets blurred only at a few combinations of embedding dimensions for high noise levels and short time series. This is because the variance of the estimated measures increases with the embedding dimension and the noise level. Thus for small coupling strengths, the distribution of the measures in the two directions may overlap and suggest no discrimination in the two directions.

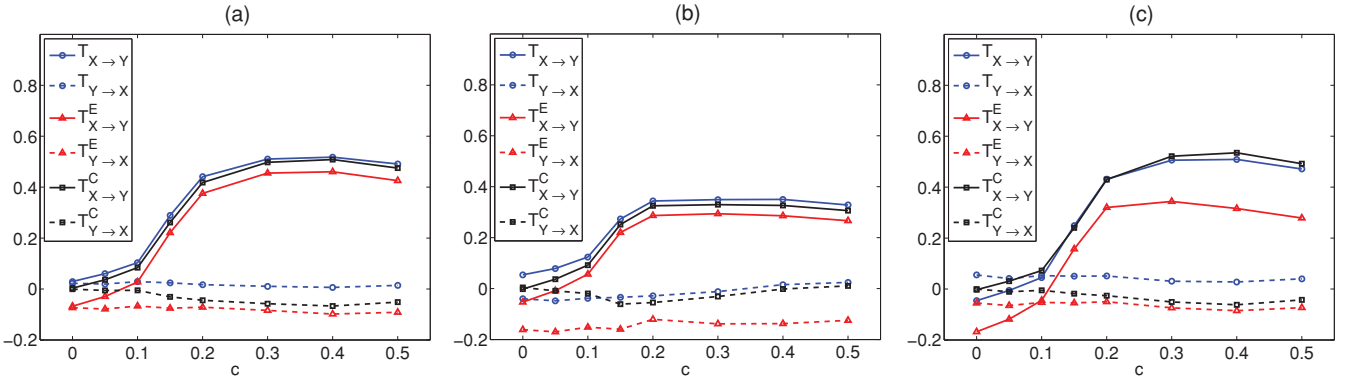

FIG. 2. (Color online) (a) Mean estimated values of TE (T), ETE (T^E), and CTE (T^C) for both directions from 100 realizations of the noise-free unidirectionally coupled Henon maps, with $n = 512$ and $m_x = m_y = 2$. (b) and (c) are as in (a) but for $m_x = 2, m_y = 4$ and $m_x = 4, m_y = 2$, respectively.

Symbolic transfer entropy (STE) and its corrections (CSTE and ESTE) seem to be more affected by the selection of the embedding dimensions than the respective TE measures. In the presence of unidirectional coupling, STE and CSTE detect it correctly for $m_x \geqslant m_y > 2$, while ESTE is significantly affected by the embedding dimensions [see Figs. 3(a) and 3(b)]. CSTE is the least sensitive to noise and gives the most consistent results in the case of no causal effects, whereas STE is positively biased and ESTE is negatively biased [see Fig. 3(c)]. The variance of the symbolic measures is small and does not seem to increase with the addition of noise as much as for the TE measures, so that the overlap in the two directions for small coupling strength is much smaller. However, for small coupling strengths, estimated values of the symbolic measures from the two directions again overlap.

The graphical results, as those shown in Figs. 1–3, are quantified by the score of the three statistical tests. When there is no coupling, the measures MCR and CMCR reject almost always H_0^1 and H_0^2, and reject H_0^3 when $m_x = m_y$, so they always score at least 2 (see Table I). The reason for the rejections is that the measures are positively biased and have very small standard deviation, and apparently the proposed correction of MCR cannot eliminate this bias either. Though the bias decreases with the increase of the time series length, the score for MCR and CMCR is still at least 2 and the addition of noise does not change the score results. On the other hand, CTE scores 0 for all combinations of embedding dimensions, even for time-series lengths as small as $n = 512$, whereas TE does this only for large m_x, m_y and ETE always scores at least 2. CSTE also often scores 0 for $m_x, m_y > 2$, while STE and ESTE perform poorly, rejecting H_0^1 and H_0^2 mostly due to the positive and negative bias, respectively. The proper performance of CTE and CSTE is not substantially affected by the addition of noise.

For the second setting of the presence of unidirectional coupling, the measures perform rather similarly. CMCR and MCR give scores 2 or 3, meaning that in addition to H_0^1, H_0^2 is also rejected, erroneously due to positive bias, and in some cases H_0^3 is rejected as well. H_0^2 is often rejected by the information measures due to either positive bias (TE) or negative bias (ETE and sometimes CTE). ETE gives systematically negative values, while CTE might have a slightly negative mean in some cases, however its estimated values are around zero. CSTE turns out to outperform all the other measures and gives a proper score 2 (only H_0^2 is not rejected) and it is also robust against noise, even for a high level of noise (20%).

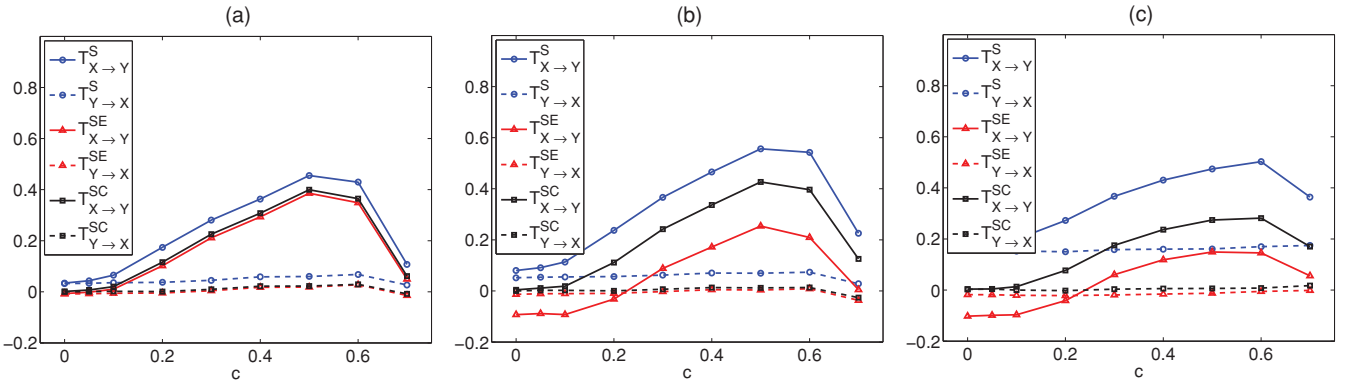

FIG. 3. (Color online) (a) Mean estimated values of STE (T^S), ESTE (T^{SE}), and CSTE (T^{SC}) for both directions from 100 realizations of the noise-free unidirectionally coupled Henon maps, with $n = 512$ and $m_x = m_y = 3$. (b) As in (a) but for $m_x = 4, m_y = 3$. (c) As in (b) but for 20% noise level.

TABLE I. Scores for the setting of no coupling from the 100 realizations of the uncoupled Henon maps with $n = 512$, for noise-free data and 20% noise (the latter values are in parentheses).

		Scores, 0% noise (20% noise)							
m_x	m_y	M	M^C	T	T^E	T^C	T^S	T^{SE}	T^{SC}
2	2	2(2)	2(2)	2(2)	2(0)	0(0)	2(2)	1(0)	1(0)
2	3	3(3)	3(3)	3(1)	3(0)	0(0)	2(3)	0(0)	1(0)
2	4	3(3)	3(3)	3(2)	3(2)	0(0)	3(2)	2(3)	1(1)
2	5	3(3)	3(3)	3(2)	3(2)	0(0)	2(3)	2(2)	0(0)
3	2	3(3)	3(3)	3(0)	3(0)	0(1)	2(2)	2(0)	3(0)
3	3	2(2)	2(2)	2(0)	2(0)	0(0)	2(2)	2(2)	0(0)
3	4	3(3)	3(3)	2(0)	3(3)	0(0)	2(3)	2(3)	0(0)
3	5	3(3)	3(3)	3(0)	3(3)	0(0)	3(3)	3(3)	0(0)
4	2	3(3)	3(3)	3(0)	3(2)	0(1)	3(2)	3(2)	0(1)
4	3	3(3)	3(3)	2(2)	3(3)	0(1)	3(3)	2(3)	2(0)
4	4	2(2)	2(2)	0(0)	2(2)	0(0)	2(2)	2(2)	0(0)
4	5	3(3)	3(3)	0(2)	3(2)	0(2)	3(2)	3(3)	0(0)
5	2	3(3)	3(3)	3(2)	3(3)	0(1)	2(3)	2(2)	1(0)
5	3	3(3)	3(3)	3(0)	3(3)	0(0)	3(3)	3(3)	2(0)
5	4	3(3)	3(3)	0(0)	3(2)	0(2)	3(2)	3(3)	0(0)
5	5	3(2)	3(2)	0(2)	2(0)	0(2)	2(2)	2(3)	0(2)

C. Results on the unidirectionally coupled Mackey-Glass systems

For the unidirectionally coupled Mackey-Glass systems, the MCR measures increase also in the opposite direction with the coupling strength for all embedding dimensions. The MCR and CMCR values are larger in the correct direction only for $m_x \leqslant m_y$, whereas for $m_x = m_y$ they increase close together in both directions (see Fig. 4). The addition of noise worsens the performance of the MCR measures. It is notable that for $\Delta_x = \Delta_y$, MCR and CMCR point to the wrong direction of interaction.

The transfer entropy measures are also significantly affected by the embedding dimension. The direction of the causal effect is generally detected with all measures when $m_x \geqslant m_y$, but fails when m_x is much smaller than m_y. For example, for $\Delta_x = 30$ and $\Delta_y = 100$, all measures detect the correct driving effect when $m_x \geqslant m_y$, as shown in Fig. 5(a) for $m_x = 4$, $m_y = 3$, contrary to the MCR measures shown for the same setup in Fig. 4(b). For systems with $\Delta_x = \Delta_y$, the detection is problematic even for $m_x = m_y$, and the stronger the coupling, the larger $m_x = m_y$ is needed to be detected. This feature is shown in Figs. 5(c) and 5(d) for $\Delta_x = \Delta_y = 17$, where $T_{X\to Y} > T_{Y\to X}$ holds only for very weak coupling when $m_x = m_y = 3$ [see Fig. 5(c)], and in order to achieve $T_{X\to Y} > T_{Y\to X}$ also for stronger coupling $m_x = m_y$ has to be increased to 5 [see Fig. 5(d)]. In all cases, TE, CTE, and ETE show the same signature (almost parallel lines in Fig. 5), but CTE attains best the zero level at $c = 0$, whereas TE is slightly positively biased for certain embedding dimensions and ETE is negatively biased. The addition of noise does not change these structures but decreases their mean value and increases their variance, particularly for large embedding dimensions [see Fig. 5(b)].

The symbolic transfer entropy measures depend on the embedding dimensions more than the transfer entropy measures, and fail more often to detect the correct causal effect, as can be seen from the comparison of the results on TE measures in Figs. 5(a)–5(c) and STE measures in Fig. 6 for the same simulation setup. However, CSTE gives values around zero for any selection of embedding dimensions in the case of no causal effects.

Regarding the formal hypothesis tests, for the uncoupled Mackey-Glass systems, MCR and CMCR scored high in the first setting of no coupling and rejected almost always H_0^1 and H_0^2 for the Mackey-Glass system (see Table II for $\Delta_x = 17$, $\Delta_y = 30$, and $m_x = m_y$). CTE and CSTE scored worse overall than for the Henon map, but still better than their respective counterparts, TE, ETE and STE, ESTE, respectively. For example, for $\Delta_x = 30$ and $\Delta_y = 100$, CSTE scored 0 in most of the combinations of m_x and m_y, while the other information measures performed poorly, scoring mostly 3 or 2.

For all scenarios of complexity of the coupled Mackey-Glass systems, STE obtains significant positive values also for $c = 0$ when $m_x < m_y$, while ESTE obtains often negative values. CSTE follows the same dependence on c as STE but

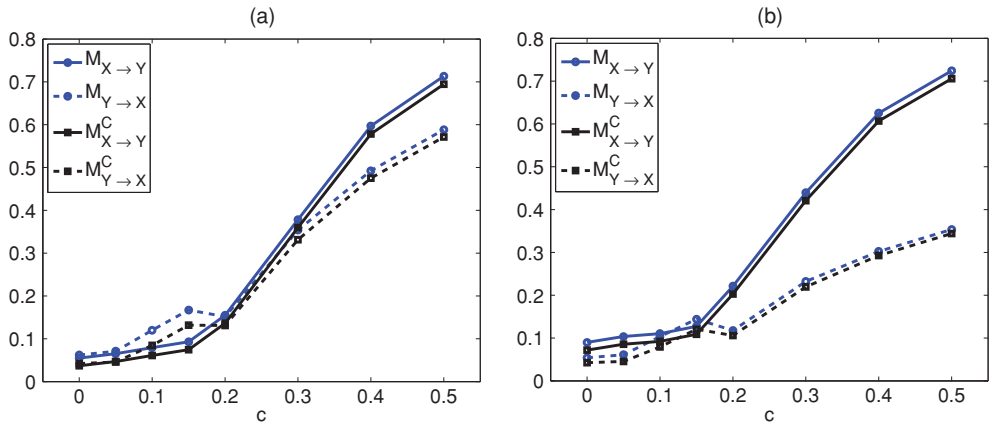

FIG. 4. (Color online) (a) Mean estimated values of MCR (M) and CMCR (M^C) for both directions from 100 realizations of the noise-free unidirectionally coupled Mackey-Glass systems with $\Delta_x = 30$ and $\Delta_y = 100$, $n = 2048$, and $m_x = m_y = 3$. (b) As in (a) but for $m_x = 4, m_y = 3$.

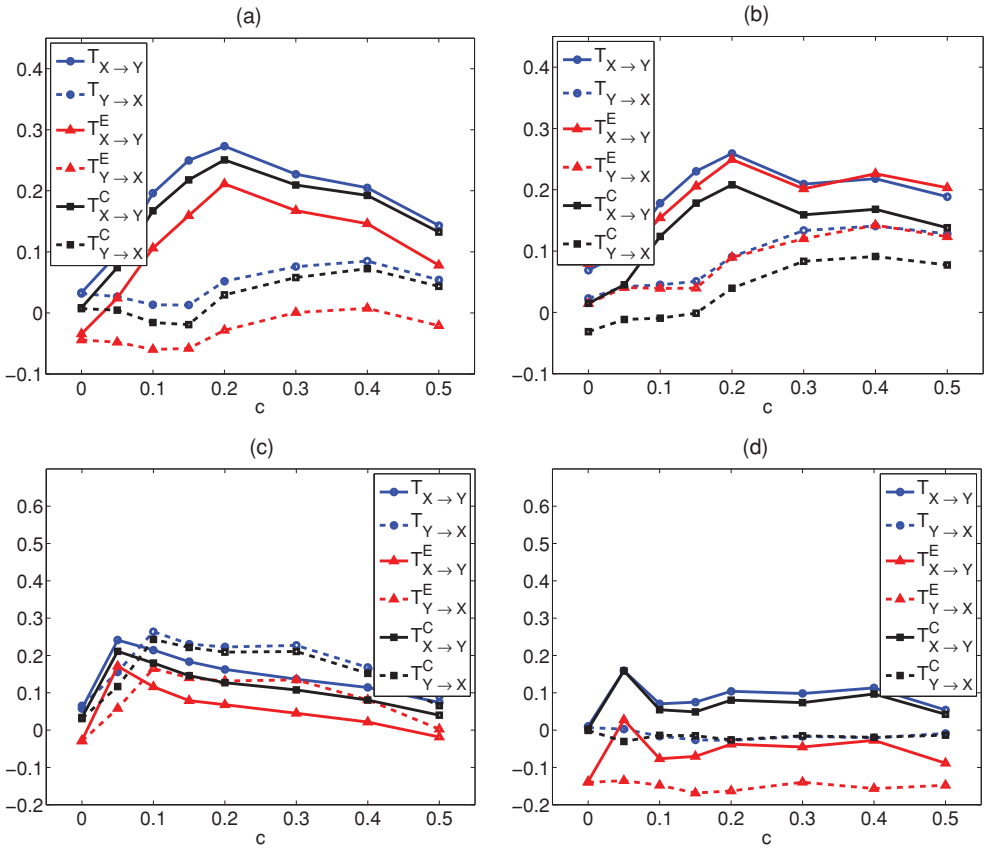

FIG. 5. (Color online) (a) Mean estimated values of TE (T), ETE (T^E), and CTE (T^C) for both directions from 100 realizations of the noise-free unidirectionally coupled Mackey-Glass systems ($\Delta_x = 30$, $\Delta_y = 100$) with $n = 2048$ and $m_x = 4$ and $m_y = 3$. (b) As in (a) but for 20% noise level. (c) and (d) As in (a) but for $\Delta_x = \Delta_y = 17$, $m_x = m_y = 3$, and $m_x = m_y = 5$, respectively.

is displaced so that CSTE falls at the zero level for $c = 0$. It is interesting that in the presence of noise, STE gets even larger values for $c = 0$ and increases faster for $c > 0$, and CSTE has the same course with c as STE but starts at the zero level for $c = 0$. We illustrate this nice property of CTE and CSTE for $c = 0$ as a function of m_x, where $m_x = m_y$ in Fig. 7. First, we note that STE measures have much less variance than the respective TE measures and attain the zero level for small $m_x = m_y$ [in Fig. 7(a), only the distribution of CTE contains zero for varying $m_x = m_y$]. In Fig. 7(c), where the systems have different complexity, ETE gets more affected by the individual system complexity as the embedding dimension increases; TE and CTE do not differ much in the two directions, but only CTE is at the zero level.

In the presence of unidirectional coupling, MCR and CMCR score at least 2 as the first and second H_0 are rejected, meaning that the measures are positively biased and the estimated values of the measures increase at the same level in both directions. The latter does not occur with the information measures, and H_0^3 is almost always rejected, as well as H_0^1

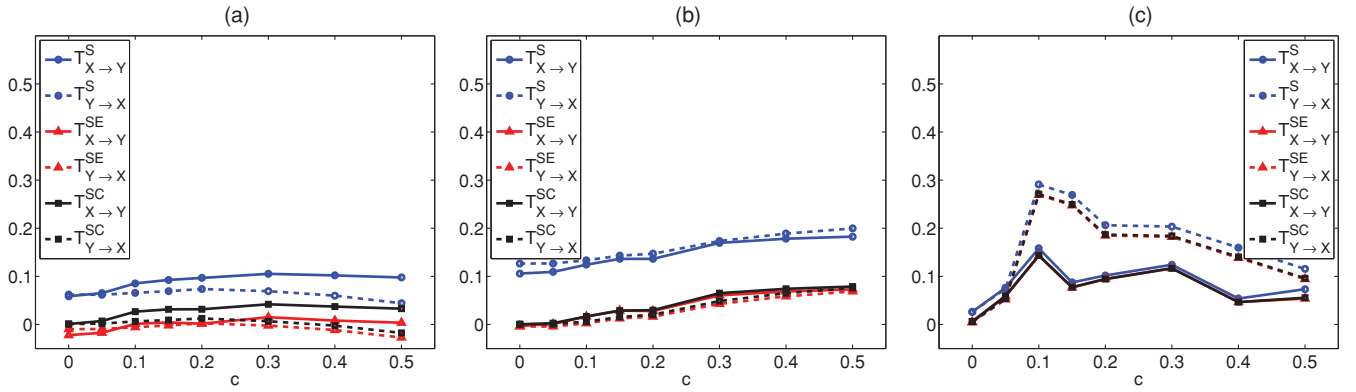

FIG. 6. (Color online) The panels are as for the first three panels of Fig. 5 but for the symbolic transfer entropy measures.

TABLE II. Scores for the setting of no coupling of the information measures, from the 100 realizations of the uncoupled Mackey-Glass system ($\Delta_x = 17$, $\Delta_y = 30$) with $n = 2048$, for the noise-free case and for 20% noise level.

	Scores, 0% noise (20% noise)							
$m_x = m_y$	M	M^C	T	T^E	T^C	T^S	T^{SE}	T^{SC}
2	3(3)	3(3)	3(2)	3(0)	3(0)	2(2)	2(0)	2(0)
3	3(3)	3(3)	2(2)	3(0)	2(0)	2(2)	2(0)	2(0)
4	3(3)	3(3)	2(0)	3(2)	0(0)	3(3)	3(3)	1(1)
5	3(3)	3(3)	2(0)	3(3)	0(0)	3(3)	3(3)	0(0)
6	3(3)	3(3)	2(1)	3(2)	1(1)	3(3)	3(3)	1(0)
7	3(3)	3(3)	1(2)	3(2)	1(2)	3(2)	3(3)	1(0)

(the correct direction of coupling). In this task, the corrected measures (CTE and CSTE) performed similarly to the original measures.

The simulations on the coupled Mackey-Glass systems showed that CTE and CSTE improve the performance of the original measures, giving values closer to zero when the systems are uncoupled. Similarly to the coupled Henon maps, the optimal selection for embedding dimensions is $m_x = m_y$. For $m_x > m_y$, the dynamics of the driving system are overrepresented, giving larger TE and STE values in the correct direction, whereas for $m_x < m_y$ the opposite effect is observed decreasing TE and STE for $X \to Y$ and increasing TE and STE for $Y \to X$, so that for very small m_x, the measure values are even larger for the wrong direction $Y \to X$. Though CTE and CSTE decrease the positive bias due to an uneven representation of the systems when $m_x \neq m_y$, they cannot remove it completely. Another bias that cannot be eliminated by the correction of the transfer entropy measures is due to the individual dynamics, which persist for $m_x = m_y$. The bias turns out to be larger when the two systems have identical individual dynamics, i.e., $\Delta_x = \Delta_y$. We found that for all three $\Delta_x = \Delta_y$ values we tested for, only small coupling strength c could be detected correctly using small $m_x = m_y$, and for larger c the embedding dimension should be increased with the complication that it may be too large for the given time-series length. We attribute this to the similarity of the trajectories of the driving and response system, even when they are not in phase, so that a larger time window length from each trajectory is required to detect differences (in terms of entropies) that reveal the driving effect. When $\Delta_x \neq \Delta_y$, as driving increases, the shape of the trajectories of the response system gets closer to that of the driving system, and therefore the driving effect can be detected better even for small $m_x = m_y$. Indeed, this was the case for all combinations of $\Delta = 100$ and any of $\Delta = 17, 30$ (at any order of driving and response). For the pair $(\Delta_x = 17, \Delta_y = 30)$, the difference in the individual dynamics was smaller and the detection of the correct driving effect for $c > 0.2$ required that $m_x = m_y$ be as large as 6, while for the pair $(\Delta_x = 30, \Delta_y = 17)$ even larger $m_x = m_y$ was required.

D. Results on the coupled nonlinear stochastic system

For the coupled nonlinear stochastic system of three variables, the driving effects $X \to Y$, $Y \to Z$, and $X \to Z$ take place at lag one, so we expect that $m_x = m_y = 1$ will be sufficient for all pairs of variables. However, MCR gives larger values at the correct driving effect $X \to Y$ (meaning any of $X \to Y$, $Y \to Z$, and $X \to Z$) for larger embedding dimensions $m_x \geqslant m_y$ and with a large bias that decreases with the increase of time-series length. CMCR reduces the MCR values but does not attain the zero level when evaluated for no coupling or an opposite driving effect.

TE is also positively biased for all embedding dimensions, and one can only observe the correct driving from the relative difference in the two directions. Though TE decreases with the increase of time-series length, it stays positive also for the opposite driving effect [for the pair (X,Y) of the stochastic systems, see Fig. 8(a) for $m_x = m_y = 1$ and Fig. 8(c) for $m_x = m_y = 2$]. CTE resolves this problem by reducing the bias in both directions so that CTE for the opposite driving effect is at the zero level [Fig. 8(b) for $m_x = m_y = 1$ and Fig. 8(d) for $m_x = m_y = 2$]. Note that for $m_x = m_y = 1$, CTE reduces to ETE, whereas for $m_x = m_y = 2$, ETE is different and becomes negative, obtaining a smaller relative difference

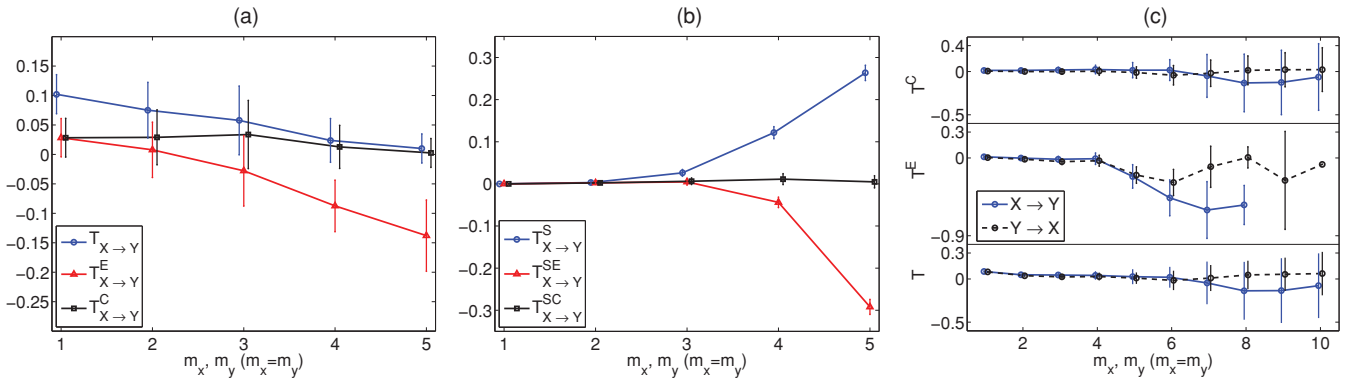

FIG. 7. (Color online) (a) Mean TE (T), ETE (T^E), and CTE (T^C) (error bars denote the standard deviation) from 100 realizations of the noise-free uncoupled Mackey-Glass systems with $\Delta_1 = \Delta_2 = 17$, $n = 2048$, and for varying $m_x = m_y$. Only the one direction is shown as the two systems are the same. (b) As in (a) but for STE, ESTE, and CTE. (c) As in (a) but for $\Delta_1 = 30, \Delta_2 = 100$; the two directions are shown, as given in the legend, with a measure at each panel. The drawn points and error bars for each measure are slightly displaced along the x axis to facilitate visualization.

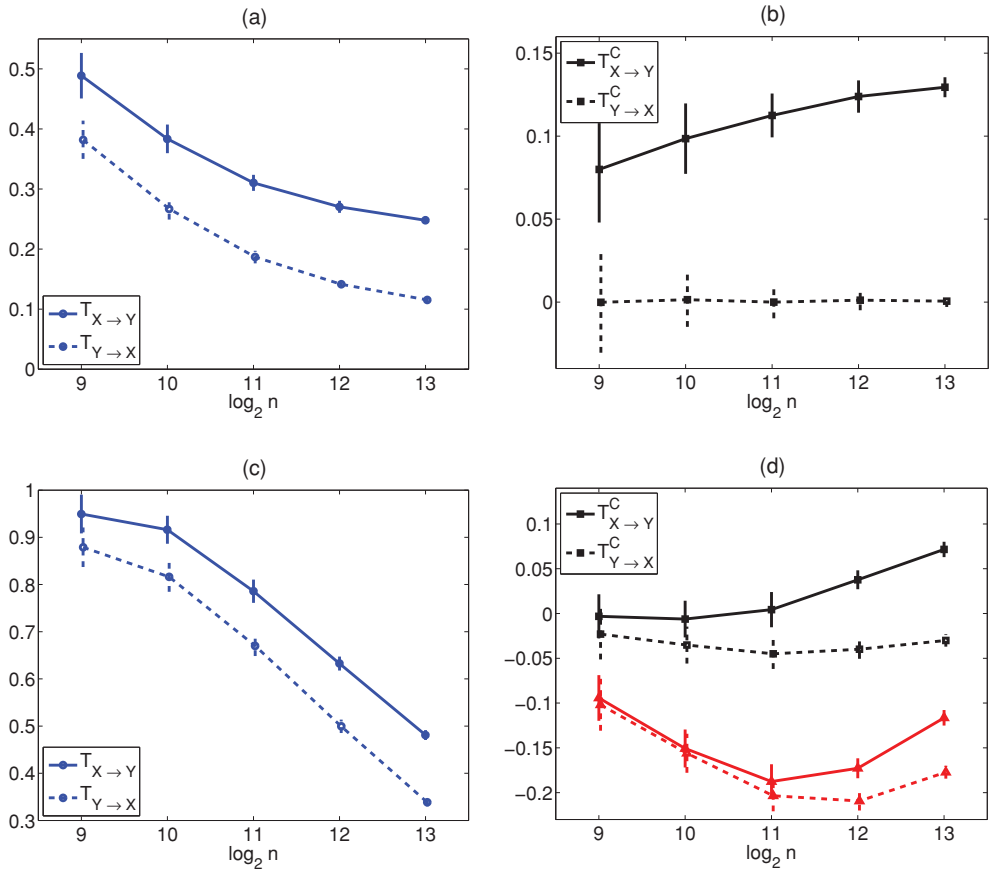

FIG. 8. (Color online) Mean TE (T) (error bars denote the standard deviation) from 100 realizations of the coupled stochastic system vs time-series length $\log_2 n$, for the variables X and Y, and $m_x = m_y = 1$. (b) As in (a) but for CTE (T^C). (c) As in (a) but for $m_x = m_y = 2$. (d) As in (b) but for CTE (T^C) and ETE (T^E) and $m_x = m_y = 2$. The drawn points and error bars for each measure are slightly displaced along the x axis to facilitate visualization.

between the two directions than for the other systems. The same results are observed for the other two variable pairs.

The situation with STE and its correction is similar to TE, but starting at $m_x = m_y = 2$, with the only difference being that for the pair (X, Z), the correct driving $X \to Z$ is less evident as for this case it is nonlinear and weaker.

E. Comparison to other types of surrogates

We compare the corrected measures defined in terms of random shuffling of the reconstructed points to other surrogates data schemes, i.e., twin surrogates [30] and time-shifted surrogates [13]. We concentrate on the TE measure, but our simulations with STE produced similar results. Measures using the twin or time-shifted surrogates are estimated as the difference of TE on the original bivariate time series and the mean TE on M surrogates. CTE turns out to perform the same as for the two types of surrogates, or even better in some cases. Although all three measures (using shuffled reconstructed vectors, twin surrogates, and time-shifted surrogates) establish the zero level for the direction $Y \to X$, CTE is larger for $X \to Y$ for the whole range of $c > 0$. Representative examples are given in Fig. 9 for the time-shifted surrogates and the Mackey-Glass system. We note here that twin surrogates have the highest computational cost because of the long computation time in constructing the surrogates.

V. APPLICATION TO EEG

The measures considered in the simulation study are evaluated on two scalp preictal EEG records of 25 channels (system 10–20 with added low rows) and one intracranial EEG preictal record of 28 channels in a grid. We want to evaluate how the measures detect changes in the interactions of any pair of channels from the early to the late preictal state. The first extracranial EEG record is for a generalized tonic clonic seizure, and the other is for a left back temporal lobe epilepsy. No specific artifact removal method was applied, but to attain better source derivation at small cortical regions, for each EEG channel, the mean EEG of the four neighboring channels was subtracted [36]. The pairs of transformed EEG that were used for the estimation of the measures are as follows: central left (C3) versus right (C4), temporal left (T7) versus right (T8), frontal left (F3) versus right (F4), and parietal left (P3) versus right (P4). For the intracranial EEG, the pairs of channels were either from the same brain area [two left frontal (LTP-1 versus LTP-3), two left temporal (LST-1 versus LST-3), two left occipital channels (ROT-1 versus ROT-3) and the same for the right side (RTP-1 versus RTP-3, RST-1 versus RST-3,

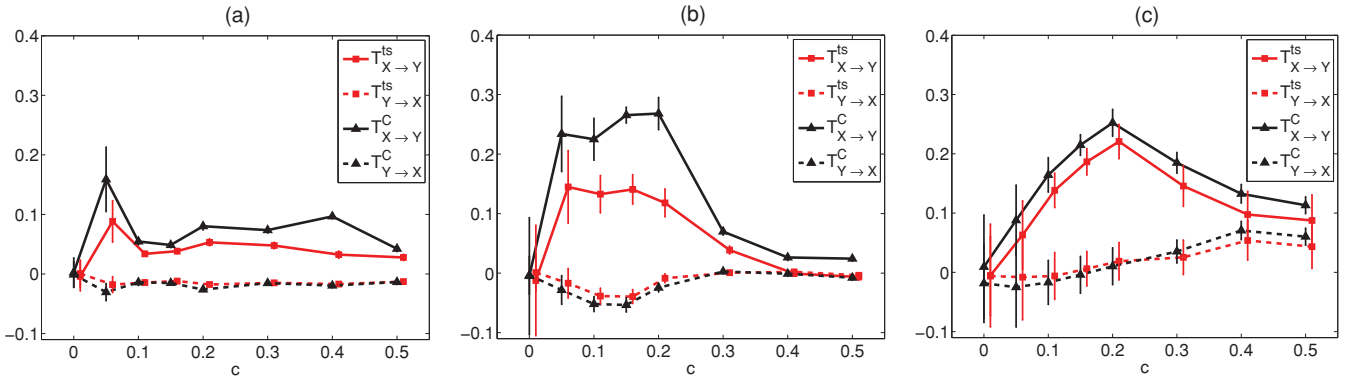

FIG. 9. (Color online) (a)Mean CTE (T^C) and TE from the time-shifted surrogates, denoted as T^{ts} (error bars denote the standard deviation) from 100 realizations of the noise-free Mackey-Glass systems with $\Delta_1 = \Delta_2 = 17$, $n = 2048$, and for $m_x = m_y = 5$. (b) and (c) are as (a) but for $\Delta_1 = 17, \Delta_2 = 30$ and $\Delta_1 = 30, \Delta_2 = 100$, respectively. The curves and error bars for each measure are slightly displaced along the x axis to facilitate visualization.

ROT-1 versus ROT-3)], or from opposite brain areas [a left and right frontal (LTP-1 versus RTP-1), temporal (LST-1 versus RST-1), and occipital channels (LOT-1 versus ROT-1)].

The data windows are from 4 to 3 h before the seizure onset (early preictal state) and the last 1 h before the seizure onset (late preictal state). Each 1-h-long data window is split to 120 successive nonoverlapping segments of 30 s, and the causality measures are estimated for the channel pairs at each segment and for both directions. As the sampling frequency is 100 Hz, each 30-s segment consists of 3000 data points. For an estimation of the measures, the embedding dimensions are $m_x = m_y = 3$ and $m_x = m_y = 5$, the time horizon is $h = 5$, the lags are $\tau_x = \tau_y = 5$, and the radius is $r = 0.2$ times the standard deviation of the data.

The causality measures indicate a bidirectional form of information flow among most of the brain areas, and this is present at both preictal states. Only a few causality measures detect a slight change in the information flow between the early and late preictal state. The increase of m_x,m_y from 3 to 5 decreases the measure values, as expected also from the simulation study [see, e.g., Figs. 10(a) and 10(b) for the MCR measures]. Corrected measures, as expected, give lower values than the original measures. For the same example, CMCR shown in Fig. 10(c) drops to the zero level for most of the segments, regardless of the state, which shows that the interaction observed by MCR may be attributed to bias in the estimation that originates from the individual system dynamics and state space reconstruction. A similar drop is observed for the corrected information measures, as shown in Figs. 10(d) and 10(e) for TE and CTE, respectively.

There is no consistent result from all measures for the direction of the interdependence. For example, for the pair of channels (C3,C4) and for the first seizure, MCR measures suggest that C3 drives C4, but not CMCR, as shown in Fig. 10, whereas the information measures indicate a bidirectional coupling. STE in particular, for $m_x = m_y = 5$, manifests an abrupt drop just shortly before the seizure onset for all pairs of channels [see Fig. 11(a) for channels C3,C4]. CSTE renders this drop, giving values around zero for all times [see Fig. 11(b)].

For the second seizure of temporal lobe type, a significant change in the interdependence between the two preictal states could not be observed, at least for the selected pairs of channels. Bidirectional coupling is suggested by the original measures at both states, whereas the corrected measures again give values around zero. TE and CTE were rather unstable, exhibiting large fluctuations across the successive segments of each preictal state. Moreover, they had computational problems and they could not always be calculated when $m_x = m_y \geqslant 5$ (the correlation sum contained zero terms due to a lack of close neighboring points).

Although intracranial EEG are less noisy, no clear indication of change in the causal effects between early and late preictal states could be observed as well. Corrected measures again gave values lower than the original measures (see Fig. 12), and call into question the coupling detected by the original measures.

VI. DISCUSSION

The estimation of the strength and direction of interaction in coupled systems from limited and possibly noisy bivariate time series was shown to encounter a number of problems regardless of the employed measure. It was shown that the coupling measures are affected by a number of factors, including individual system complexity, state space reconstruction, time-series length, and noise. These factors add bias to the estimation of the strength of coupling that may not be the same in both directions.

We concentrated on reducing the bias in each component of the causality measures of mean conditional recurrence (MCR), transfer entropy (TE), and symbolic transfer entropy (STE). Since there are diverse sources of bias, we attempted to account for all of them by assuming the value of each component measure when the systems are not coupled. For this, we developed the idea of surrogate data and we randomly shuffled the points of the reconstructed state space trajectory of the driving system. Considering the decomposition of each measure to component quantities, for each component the average on an ensemble of realizations of the surrogate driving trajectory was computed and subtracted from the respective original component value. Replacing the corrected components in the expression of the coupling measure, some of the bias is

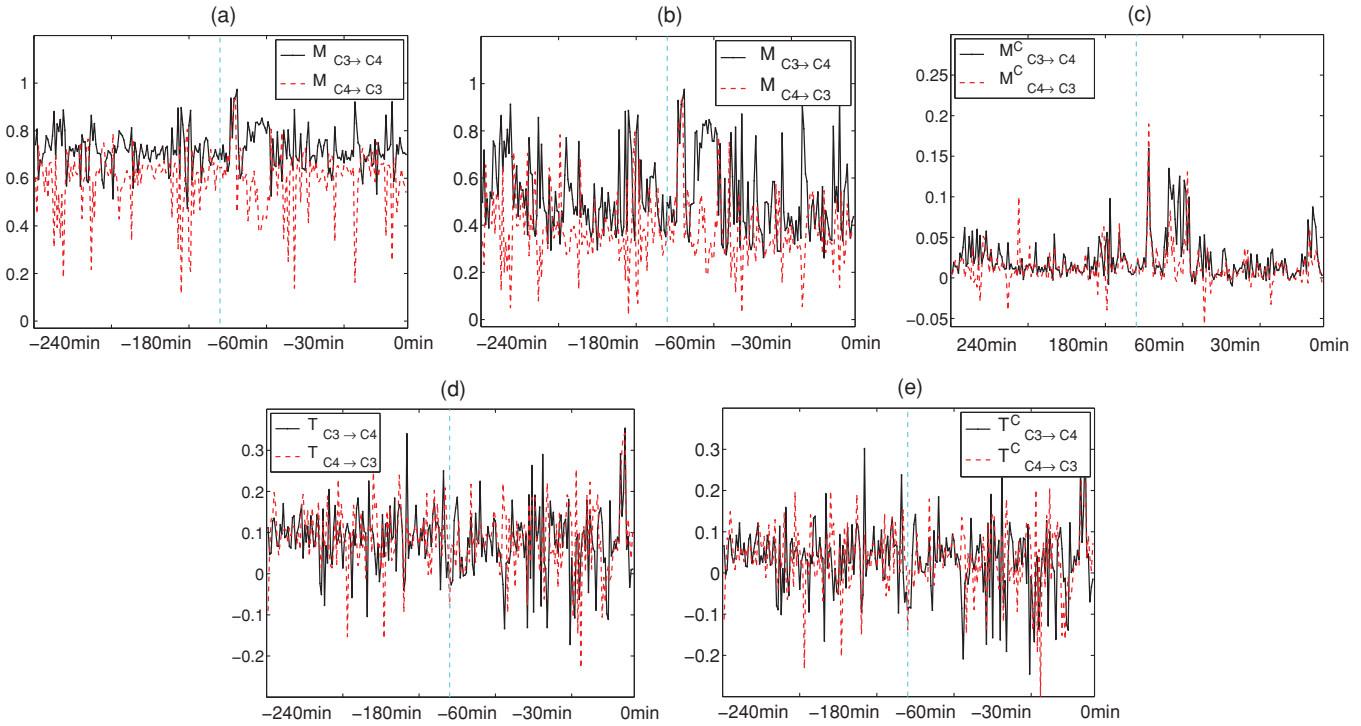

FIG. 10. (Color online) (a) MCR profiles (M) from both states (early and late preictal) of the first seizure and both directions, for channels as in the caption, with $m_x = m_y = 3$. (b) As in (a) but for $m_x = m_y = 5$. (c), (d), and (e) are as in (a) but for CMCR (M^C), TE (T), and CTE (T^C), respectively. The preictal periods are indicated by the time in minutes, with reference to time 0 at seizure onset, and they are separated by a vertical dashed line.

removed. The proposed corrected measure indeed performed as expected in simulations, but the amount of reduction of the bias varied with the measure: for MCR, the reduction with the corrected MCR (CMCR) was small in most simulations, whereas it was much larger in the application on epileptic EEG; for TE and STE, the reduction was larger and in most cases effective, so that the corrected measures, CTE and CSTE, respectively, were at the zero level in the absence of coupling.

One could argue that it is intuitively more appropriate to compute first the coupling measure on the surrogate realizations and then take the average, instead of taking the average of the components in the measure expression. For example, in the computation of CTE, we take the average of the correlation sums in Eq. (4) over all surrogates, while one would expect to take the average of the whole expression for TE, which would be equivalent to taking averages of the logarithms of the correlation sums. The latter gives more variable estimates of TE on the surrogates, as for small values of the correlation sums we obtain large negative logarithms. Indeed, our simulations showed that this version of CTE produces more varying results encountering also large negative values for some realizations.

The main advantage with the corrected measures is that they establish significance, meaning that they do not indicate

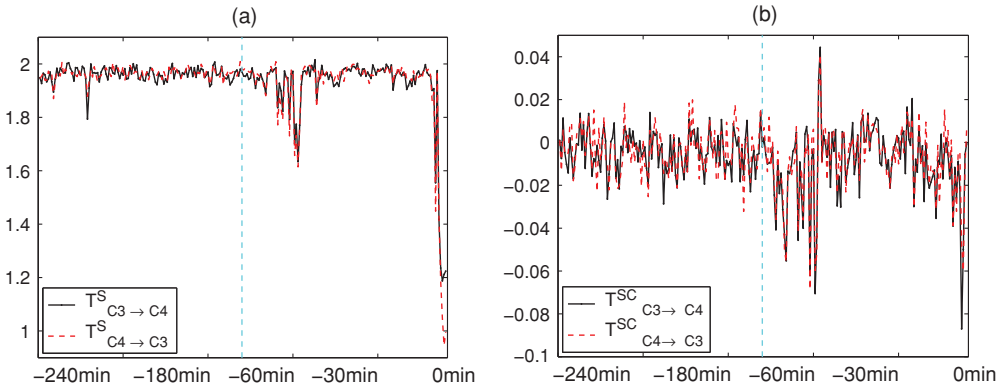

FIG. 11. (Color online) (a) STE profiles (T^S) from both states (early and late preictal) of the first seizure and both directions, for channels as in the inset, with $m_x = m_y = 5$. (b) As in (a) but for CSTE (T^{SC}).

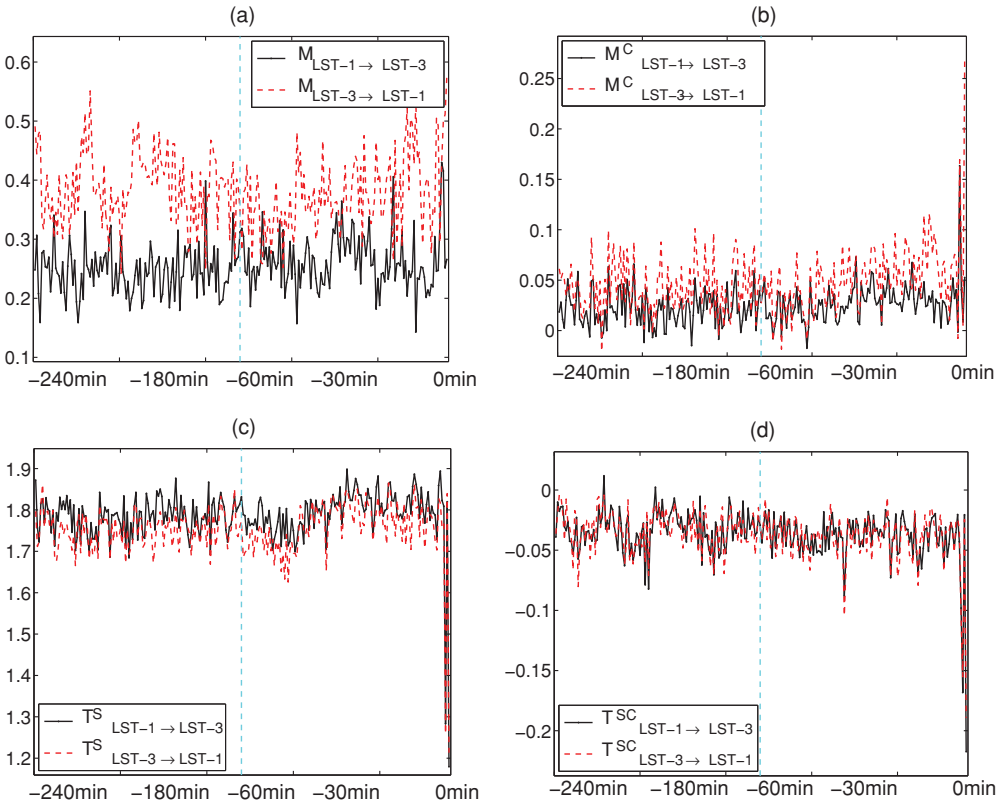

FIG. 12. (Color online) (a) MCR profiles (M) from both states (early and late preictal) and both directions of the intracranial data, for channels as in the inset, with $m_x = m_y = 5$. (b), (c), and (d) are as in (a) but for CMCR (M^C), STE (T^C), and CSTE (T^{SC}), respectively.

significant coupling when it is not there. This has been shown with all tested measures, CMCR, CTE, and CSTE, and for varying conditions of system complexity (Henon maps and Mackey-Glass of varying complexity), state space reconstruction (a range of embedding dimensions), time-series length, and noise. For TE and STE, we considered also the so-called "effective" measures, denoted ETE and ESTE, respectively, which use a similar surrogate approach, but the random shuffling is done on the samples of the time series. The simulation results showed that this approach gives a varying estimation of strength and direction of coupling that often does not correspond to the real coupling. The use of twin surrogates or time-shifted surrogates gives the same or worse results compared to the suggested corrected measures.

The performance of the measures was also assessed by statistical testing, where the samples for each test were the values of the measure on a number of realizations. CTE and CSTE were consistently found to be statistically insignificant in both directions in the absence of coupling, as opposed to the original TE and STE, as well as ETE and ESTE. In the presence of a causal effect, CTE and CSTE could identify it with the same statistical significance as TE and STE, respectively. The correction of MCR also improved the statistical results, but not as clearly as for the information measures. Comparing CTE and CSTE, the simulations showed that CSTE was more dependent on the selection of the embedding dimensions but more robust against noise.

TE, and subsequently CTE, have computational problems when the embedding dimension is large, at least when correlation sums are used for their estimation, because stable statistics on neighborhoods within a given distance cannot be established when the state space dimension is large. This was found to be the case for the application to EEG when the embedding dimension was larger than 5, where TE and CTE fluctuated a lot on successive segments of pairs of EEG channels. On the other hand, STE and CSTE were stable, and in many cases CSTE provided values close to zero, whereas STE was always larger. CMCR also gave significantly reduced values compared to MCR, but not at the zero level. Interpreting these results in view of the simulation results, CSTE was the most conservative in giving evidence for coupling, but most reliable as well, so that when coupling was actually indicated by CSTE it would be likely to be true coupling. We could not find any clear evidence that there exists a particular spatial structure of coupling at the different cortical regions we tested, or that there is a change of the coupling structure from an early preictal to a late preictal state, at least on the three EEG records we studied.

ACKNOWLEDGMENTS

We would like to thank Ralph Andrzejak for fruitful discussions and suggestions on this work.

[1] K. Hlavácková-Schindler, M. Paluš, M. Vejmelka, and J. Bhattacharya, Phys. Rep. **441**, 1 (2007).
[2] A. Arenas, A. Di'az-Guilera, J. Kurths, Y. Moreno, and C. Zhou, Phys. Rep. **469**, 93 (2008).
[3] J. F. Donges, Y. Zou, N. Marwan, and J. Kurths, Europhys. Lett. **87**, 48007 (2009).
[4] D. A. Smirnov and I. I. Mokhov, Phys. Rev. E **80**, 016208 (2009).
[5] B. Bezruchko, V. Ponomarenko, M. G. Rosenblum, and A. S. Pikovsky, Chaos **13**, 179 (2003).
[6] O. Kwon and J.-S. Yang, Europhys. Lett. **82**, 68003 (2008).
[7] J. Arnhold, P. Grassberger, K. Lehnertz, and C. E. Elger, Physica D **134**, 419 (1999).
[8] M. Dhamala, G. Rangarajan, and M. Ding, NeuroImage **41**, 354 (2008).
[9] J. Granger, Acta Phys. Pol. B**37**, 424 (1969).
[10] L. Baccalá and K. Sameshima, Biol. Cybern. **84**, 463 (2001).
[11] M. Winterhalder, B. Schelter, W. Hesse, K. Schwab, L. Leistritz, D. Klan, R. Bauer, J. Timmer, and H. Witte, Signal Proc. **85**, 2137 (2005).
[12] Y. Chen, G. Rangarajan, J. Feng, and M. Ding, Phys. Lett. A **324**, 26 (2004).
[13] L. Faes, A. Porta, and G. Nollo, Phys. Rev. E **78**, 026201 (2008).
[14] M. G. Rosenblum and A. S. Pikovsky, Phys. Rev. E **64**, 045202 (2001).
[15] D. A. Smirnov and B. P. Bezruchko, Phys. Rev. E **68**, 046209 (2003).
[16] R. Quian Quiroga, J. Arnhold, and P. Grassberger, Phys. Rev. E **61**, 5142 (2000).
[17] R. G. Andrzejak, A. Kraskov, H. Stögbauer, F. Mormann, and T. Kreuz, Phys. Rev. E **68**, 066202 (2003).
[18] M. C. Romano, M. Thiel, J. Kurths, and C. Grebogi, Phys. Rev. E **76**, 036211 (2007).
[19] D. Chicharro and R. G. Andrzejak, Phys. Rev. E **80**, 026217 (2009).
[20] T. Schreiber, Phys. Rev. Lett. **85**, 461 (2000).
[21] M. Paluš, V. Komárek, T. Procházka, Z. Hrncír, and K. Sterbová, IEEE Eng. Med. Biol. Mag. **20**, 65 (2001).
[22] R. Marschinski and H. Kantz, Eur. Phys. J. B **30**, 275 (2002).
[23] M. Staniek and K. Lehnertz, Phys. Rev. Lett. **100**, 158101 (2008).
[24] M. Vejmelka and M. Paluš, Phys. Rev. E **77**, 026214 (2008).
[25] M. Paluš and M. Vejmelka, Phys. Rev. E **75**, 056211 (2007).
[26] D. A. Smirnov and R. G. Andrzejak, Phys. Rev. E **71**, 036207 (2005).
[27] M. Lungarella, K. Ishiguro, Y. Kuniyoshi, and N. Otsu, J. Bifurcation Chaos **17**, 903 (2007).
[28] T. Kreuz, F. Mormann, R. G. Andrzejak, A. Kraskov, K. Lehnertz, and P. Grassberger, Physica D **225**, 29 (2007).
[29] A. Papana and D. Kugiumtzis, in *Topics on Chaotic Systems*, selected papers from CHAOS 2008 International Conference, Chania (World Scientific, Singapore, 2008), pp. 251–264.
[30] M. Thiel, M. C. Romano, J. Kurths, M. Rolfs, and R. Kliegl, Europhys. Lett. **75**, 535 (2006).
[31] J. P. Eckmann, S. O. Kamphorst, and D. Ruelle, Europhys. Lett. **4**, 973 (1987).
[32] S. Manzan and C. Diks, Studies Nonlin. Dyn. Economet. **6**, 1005 (2002).
[33] D. V. Senthilkumar, M. Lakshmanan, and J. Kurths, Chaos **18**, 023118 (2008).
[34] P. Grassberger and I. Procaccia, Physica D **9**, 189 (1983).
[35] B. Gourévitch, R. Le Bouquin-Jeannés, and G. Faucon, Biol. Cybern. **95**, 349 (2006).
[36] B. Hjorth, Electroencephalog. Clin. Neurophysiol. **39**, 512 (1975).